Journal of Materials and Electronic Devices 2 (2023) 8-14

Photodiode Characteristics of TiO:NiO Composite Thin Structures

Burhan COŞKUN[1*], Fatih ÜNAL[2], Mümin Mehmet KOÇ[1,3]

[1*] Department of Physics, Faculty of Arts and Sciences, Kırklareli University, Kırklareli, Türkiye
[2]Central Research Laboratory, Application and Research Center, Giresun University, Giresun, Turkey
[3]School of Medical Service, Department of Health Service and Techniques, Kırklareli University, Kırklareli, Türkiye

TiO:NiO suspension was prepared prior to thin film production. The suspension was prepared 1:1 molar rate which was produced using sol-gel method. The suspension was then spin-coated on p-type Si wafers. I-V (current - voltage) characteristics of the composite thin films were investigated in the dark and under different illumination intensities. Current - voltage graphs of the TiO:NiO composite thin films were used to determine the photovoltaic characteristics. Three different methods (Ohms Law, Thermionic Emission Theory, and Cheung& Cheung Theory) were used to assess the photodiode characteristics of the composite thin films. In the photodiode characterization, different parameters like series resistance, barrier height, Shunt resistance, ideality factor, etc. were determined. İllumination related characteristics like I_{ph} and photoresponsivity characteristics were also investigated in this work. It was seen that TiO:NiO composite thin films were affected by illumination intensities where illumination-dependent diode characteristics were evidenced in the work.

Keywords: *Photodiodes; TiO;NiO; Thin Films; Composite Thin Films; I-V; TiO*

Submission Date: 11 March 2023
Acceptance Date: 12 June 2023

**Corresponding author: burhan.coskun@klu.edu.tr*

1. Introduction

Thin films and 2D structures are essential parts and driving forces of emerging technologies [1–3]. Advancement in efficiency for different applications such as sensors, displays, detectors, etc. was achieved with thin films. Various types of materials were used in such technologies and applications [4–6]. Organic films are one of the emerging materials which as applied to the different electronic applications regarding their potential. They were reliable, cheap and easily applicable. They are mostly consisting of organic molecules such as hydrogen, oxygen, carbon and nitrogen. Depending on their organic structure they can have different material properties with different electronic, optic and optoelectronic properties. They mostly exhibit flexible properties. Therefore, are used in flexible electronic applications. However, the stability of the materials can be a problem for users. Since they are consisting of organic molecules, they can easily be affected by external factors such as heat, humidity, excessive light, UV light, scratches, shears etc. Moreover, different chemicals such as alcohols, acids, etc can also deteriorate the overall performance of the materials [7–9]. On the other hand, metal-based compounds were found to be more durable and resistant. They exhibit high shear and scratch resistance against external factors They also exhibit excellent electrical, magnetic and optoelectronic characteristics [10–15].

Different types of metals could be found in nature; each of them illustrates different characteristics and properties. Among those, transition metals are quite interesting where astonishing electrical and catalytical properties were evidenced. Ti, Ag, Cu, Au, Fe, Ni, Co Cr, Zn, Cd, etc. are some important transition metals. Such metals have good

electron affinity. They were also used in different applications. For example, Ti, Zn, and Cd based materials were vastly used in optoelectronic, photovoltaic applications [16–18]. Ag, Cu-based materials are commonly used in catalytic and optoelectronic applications [19,20]. Fe, Ni and Co-based materials are known for their magnetic characteristics and therefore were used in different magnetic applications [11,12,21]. TiO_2, TiO-based films are vastly used in optoelectronic, photovoltaic and photodetector applications [17,22]. TiO films show low bandgap energy, and good electrical properties such properties made them a suitable candidate for solar harvesting applications [17,22]. There is a limited effort in the literature to investigate the photovoltaic and photodiode properties of Ni-based thin films. Ni-based materials exhibit magnetic characteristics and can be used in ferromagnetic and/or ferrimagnetic applications. Works investigating the catalytic and electronic properties of the Ni-based nanomaterials were also addressed in the literature [23–25]. Unfortunately, there is not a considerable effort in the literature to investigate photovoltaic and photodetector properties of Ni-based materials.

Mixing various materials help producers to get new materials with interesting properties. Mixing two or more materials ends up in obtaining composites or compounds. Mixing two or more different metals can produce composites and/or alloys. Mixing rates or metal types in a such process may alter the overall structure of the material. The process could be used to obtain tailored materials where materials with desired properties could be obtained for a specific application. For example, mixing a paramagnetic and/or diamagnetic material with ferromagnetic materials could alter the magnetic characteristics of the materials. Similarly, mixing materials with insulator characteristics with a metal could alter the electrical properties of the insulator [2,26–28]. Therefore, each composite may have unique properties.

In this manuscript, we discussed the photodiode characteristics of TiO:NiO thin films which were obtained by mixing. In our work, TiO and NiO-based solutions were produced using sol-gel synthesis and mixed with 1:1 molar ratio. The mixture was coated on a p-type Si wafer using spin coating. Al contacts were applied to the two sides of the p-Si/TiO:NiO structure where photodiode in Al/p-Si/NiO:TiO/Al structure obtained. I-V plots of the photodiodes were obtained in dark and light. Different illumination intensities were worked for the I-V plot. Diode characteristics such as barrier height, ideality factors, etc were assessed.

2. Experimental

2.1. Fabrication of TiO-doped NiO gels

TiO:NiO photodetectors were produced by sol-gel solutions which were applied onto Si wafers using the spin coating method. 10ml 2-methoxyethanol and 0.5M Titanium acetate (Ti(Ac) mixed. In another baker, 10ml 2-methoxyethanol and 0.5M Nickel (II) Chloride (Hexahydrate) were mixed. Each baker was stirred using a magnetic stirrer for 10 mins. 0.5ml of TiO solution and 0.5 ml of NiO solution were mixed where TiO:NiO solutions at 1:1 molar rate were achieved.

2.2. Fabrication of TiO:NiO Nanocomposite Thin Films

Si substrates (p-type) were chemically cleaned before the coating. In the cleaning, deionized water was used to remove residual dirt where wafers were sonicated for 5 mins. Then, sonication was continued with ethanol. Then, HF:H_2O (1:10ml) were prepared. Wafers were sonicated in an acidic solution for 5 mins. Wafers were then cleaned using pure water [29]. After the washing, wafers were N_2 blow dried. 2 cm x 2 cm substrate was cut, and 6 layers of film were coated using spin coating. The spin coating procedure was applied at 3000 rpm for 30 secs for each layer. Each layer was dried on a hot plate for 2 mins the temperature of which is 100 ˚C. When the coating procedure was finished, substrates were annealed at 420 ˚C for 1h. Then, Al contact was applied for each side of the sample. The coating was applied at 2 - 4 A˚/s evaporation rate. A total of 100 nm contact was coated on each side of the photodetectors. As a result, Al/p-Si/TiO:NiO/Al photodetectors were obtained. Al/p-Si/TiO:NiO/Al photodetectors were annealed at 570 ˚C for 5 mins under N_2 gas. FYTRONIX FY-7000 were used in the investigations. [30].

3. Results

Current-Voltage behaviours of the Al/p-Si/TiO:NiO/Al structure were investigated. The investigation was conducted between -2V and 2V under different illumination intensities. Current-Voltage plots were presented in Figure 1. In the figure, I-V results were presented for, 20mW/cm^2, 40mW/cm^2, 60mW/cm^2, 80mW/cm^2, and 100mW/cm^2 illumination intensities. I-V plots illustrate that Al/p-Si/TiO:NiO/Al structure is responsive to the light. It was seen that photocurrent was obtained for different illumination intensities. Regarding the current – voltage plot, can be seen that Al/p-Si/TiO:NiO/Al structure is responsive to the light and exhibits photodiode characteristics. In the forward bias and backward bias a difference could be seen in the same voltage value. Such a difference illustrates that

Al/p-Si/TiO:NiO/Al structure exhibits photodiode properties. The I-V graph also shows that photodiodes are responsive to applied light. It was seen that illumination intensity alteration alters the measured photocurrent. However, no apparent relation was observed between the light intensity and measured photocurrent. Using the data obtained from the I-V plot, different diode parameters like barrier height (Φ_B), ideality factor (n), series resistance (R_s), reverse saturation current, etc. were assessed. In our assessment, Cheung & Cheung method and thermionic emission theory were used.

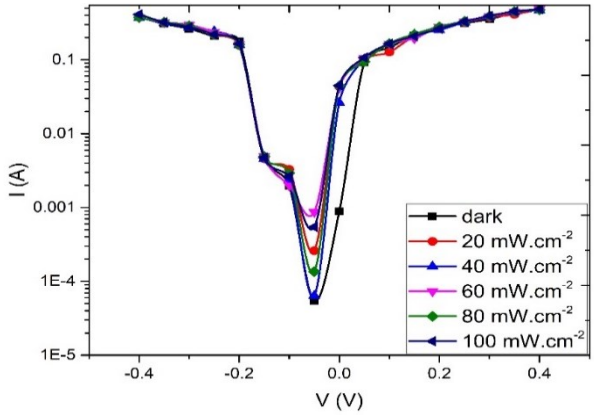

Figure 1: I-V characteristics of Al/p-Si/TiO:NiO/Al heterostructures.

In Cheung & Cheung method, the barrier height, diode resistance Rs, and ideality factor are determined using following equations:

$$\frac{dV}{d\ln(I)} = IR_s + \frac{nkT}{q} \quad (1)$$

$$H(I) = V - \frac{nkT}{q}\ln\left(\frac{I}{AA^*T^2}\right) \quad (2)$$

$$H(I) = IR_s + n\,\Phi_B \quad (3)$$

Using the equations above the graph of d(V)/d(ln(I)) and H(I) against I is drawn using the values in the low and medium voltage region of the I-V graph. Here, the ideality factor *n* was calculated using the d(V)/d(ln(I)) against I. Φ_B was derived from *n* where the curve cuts the y axis in the H(I) graph. The slope of the curve gives the R_s value.

In common Thermionic Emission theory calculations following equation was used to assess I-V plots:

$$I = AA^*T^2 \exp\left(\frac{-q\,\Phi_B}{kT}\right)\left[\exp\left(\frac{q(V-IR_S)}{kT}\right) - 1\right] \quad (4)$$

where A is the active surface area of the diode, A* is the Richardson constant, q is the charge of the electron, k is the Boltzmann constant, V is the potential, R_s is the serries resistance, T is the Kelvin temperature, Φ_B is the barrier height.

Equation 1 when $V-IR_s >> 3kT$

$$I = I_0 \exp\left(\frac{qV}{nkT}\right) \quad (5)$$

$$I_0 = AA^*T^2 \exp\left(\frac{-q\,\Phi_B}{kT}\right) \quad (6)$$

Eq 4 is obtained by taking derivative of V after taking the logarithm of Equation 3.

$$n = \frac{q}{kT}\frac{d(v)}{d(\ln(I))} \quad (7)$$

ln(I) against V in the low and medium voltage region is calculated together with other constants, the ideality factor n is found. The graph of ln(I) against V intersects ln(I) gives reverse saturation current. Here, Equation 4 gives the barrier height.

Table 1. Diode parameters obtained via thermionic emission theory.

Illumination	Ideality Factor (n)	Barrier Height (Φ_B) (eV)	Reverse saturation current I_o
0	1.10	0.58	2.84 E-5
20	2.28	0.51	0.00036
40	1.39	0.55	8.62 E-5
60	1.37	0.54	0.0001
80	2.91	0.50	0.00062
100	1.53	0.53	0.00014

Thermionic Emission Theory related diode parameters were calculated, and results were presented in Table 1. Ideality factors obtained by Thermionic Emission Theory were found between 1.10 and 2.91. It was seen that ideality factors do not increase or decrease with increasing and decreasing illumination intensity. It was seen that there is no direct relation between illumination intensity and ideality actor. A similar case was also addressed by Cheung & Cheung method . The Cheung & Cheung method provides an ideality factor between 1.38 and 3.14. The Cheung & Cheung method also could not provide a direct relation between illumination intensity and ideality factor. It was expected to obtain an ideality factor as 1 for an ideal diode.

Table 2. Diode parameters obtained via Ohm's law and Cheung & Cheung theory.

Illumination	Ohm's law		Cheung&Cheung Function	
	Rs (Ohm)	Shunt Resistance (Ohm)	Ideality Factor (n)	Rs (Ohm)
0	3.03	12.23	1.38	1.8
20	1.09	0.87	3.5	0.87
40	1.15	0.69	3.91	0.73
60	1.19	1.32	1.77	0.81
80	1.13	0.87	1.71	1.07
100	1.18	1.59	3.13	0.50

In our case, results were found to be so close to 1 for both Thermionic Emission Theory and Cheung & Cheung method. In literature different reports report ideality factor value which is bigger than 1. For example, Koc reported the ideality factor of CuO-doped carbon photodiodes 3.74. Aslan et al. find the ideality factor of ZnO-doped carbon photodiodes between 3.76 and 6.37; Ilhan et al find the ideality factor of Ti-doped CdO solar detectors between 5.75 and 7.86; Aslan et al find the ideality factor of Ti-doped amorphous carbon photodiodes as 3.17 and 1.84; Ilhan et al find the ideality factor of quaternary $CuNiSnS_4$ photodiodes as 5.84 [2,15,18,27,31]. It was seen that our results were found to be better than similar results provided in the literature. Figure 2 illustrates ideality factor and barrier height values of Al/p-Si/TiO:NiO/Al photodiodes which were obtained by the Thermionic Emission Theory.

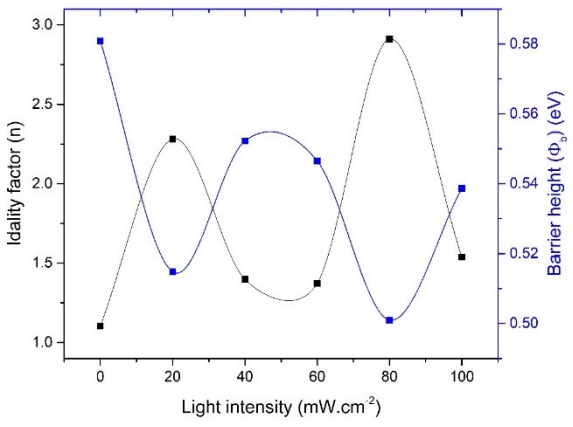

Figure 2: Ideality factors assessed by using thermionic emission theory and Cheung & Cheung method for Al/p-Si/TiO:NiO/Al photodiodes.

Using the Thermionic Emission Theory barrier height and reverse saturation current I_o were calculated and presented in Table 1. The barrier height of the Al/p-Si/TiO:NiO/Al photodiodes was found to be between 0.50 eV and 0.58 eV. The barrier height does not show a direct relation with the illumination intensity of applied light. Barrier height mostly depends on diode inner structure. Hence, various barrier height values were reported in the literature. For example, Koc reported the barrier height of CuO-doped carbon photodiodes between 0.47 eV and 0.56 eV. Aslan et al. find the barrier height of ZnO-doped carbon photodiodes between 0.48 eV and 0.56 eV. Ilhan et al find the barrier height of Ti-doped CdO solar detectors between 0.48 eV and 0.50 eV; Ilhan et al find the barrier height of quaternary $CuNiSnS_4$ photodetectors as 0.47 eV; Aslan et al find the barrier height of Ti doped amorphous carbon photodiodes as 0.46 eV and 0.56 eV; [2,15,18,27,31]. The ideality factor and barrier height of Al/p-Si/TiO:NiO/Al photodiodes were presented in Figure 2. Calculated barrier height and ideality factor values of Al/p-Si/TiO:NiO/Al photodiodes were fitting the results previously reported in the literature. Another essential and important diode parameter is reverse saturation current (I_0). It was used in the characterization of the diode. In Table 1, the reverse saturation currents were presented between 0.000028A and 0.00062 A. Altering illumination intensity alters the reverse current but no direct correlation between illumination intensity and reverse current was found for Al/p-Si/TiO:NiO/Al photodiodes. Illumination intensity-related reverse saturation current and calculated barrier height values for Al/p-Si/TiO:NiO/Al photodiodes were illustrated in Table 1 and Table 2.

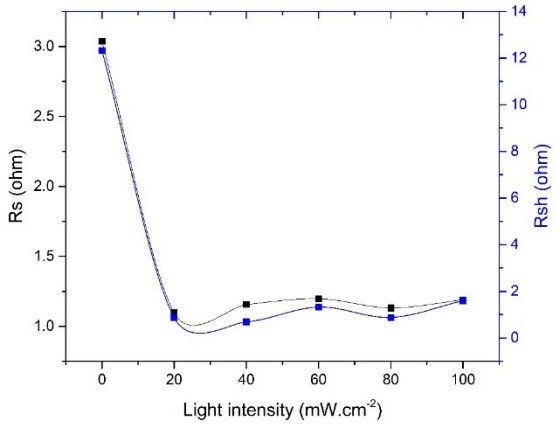

Figure 3: Calculated series resistance and Shunt resistance for Al/p-Si/TiO:NiO/Al photodiodes.

Series resistance (R_s) is an important electrical parameter for the diode which was used to characterize and identify the intrinsic properties and working parameters. They are often used to identify the diode characteristics. In this work, R_s values of Al/p-Si/TiO:NiO/Al photodetectors were obtained by Cheung & Cheung function and Ohm's law. Rs value was calculated between 1.09 Ohm and 3.03 Ohm. Relatively

lower Rs values were obtained under illumination for Al/p-Si/TiO:NiO/Al photodetectors using Ohm's law. Resistance characteristics obtained by Cheung & Cheung function were found to be similar where R_s value between 0.50 Ohm and 1.80 Ohm was calculated. R_s trend was found be quite similar. It was seen that R_s value decreases under external illumination and no illumination intensity-related derivation was observed. Light intensity-dependent R_s results obtained using two different methods were presented in Table 2.

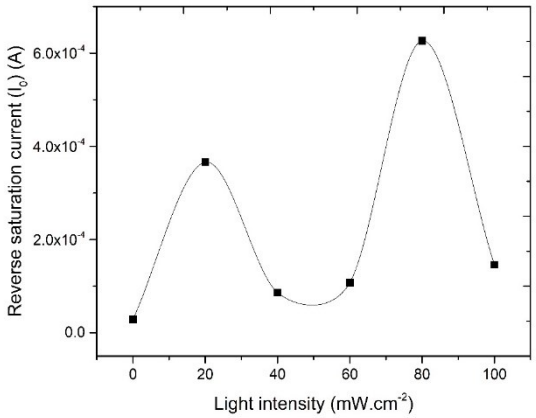

Figure 4: Light intensity dependent reverse saturation current plot for Al/p-Si/TiO:NiO/Al photodiodes.

Similar to series resistance Shunt resistance (R_{sh}) values are also critical electrical parameters for photodiodes. They are often used to identify the diode characteristics. In our work, Shunt resistance (R_{sh}) was also calculated using Ohm's law and results were presented in Figure 3. Light intensity-dependent Shunt resistance values were presented in Table 2. It was seen that Shunt resistance changed with the implication of an external light. It indicates that such characteristics is affected by light. However, no direct correlation between Shunt resistance and light intensity was observed.

Finally, the photoresponsivity and photocurrent characteristics of Al/p-Si/TiO:NiO/Al photodiodes were assessed. Results were presented in Table 3. It was seen that measured photocurrent changes with deriving illumination intensity. No direct relation between illumination intensity and measured photocurrent was seen. Similarly, photoresponsivity characteristics for the Al/p-Si/TiO:NiO/Al photodetectors were also addressed in our work. It was seen that decreasing photoresponsivity trend was observed for increasing illumination intensity We reach a conclusion that illumination intensity negatively affects the photoresponsivity for Al/p-Si/TiO:NiO/Al photodiodes. The main reason underlying such a trend may be the intrinsic structure of the photodetectors and resistive properties which were commonly be affected by external light. Such a case indicates that the intrinsic properties of our photodiodes were affected by the light.

Table 3. Light intensity related diode photosensitivity and photocurrent parameters.

I_{ph} (A)					
Volt	20 mW.cm^{-2}	40 mW.cm^{-2}	60 mW.cm^{-2}	80 mW.cm^{-2}	100 mW.cm^{-2}
-0.40000001	0.463504007	0.459108007	0.427571	0.443748007	0.415464
0.400000006	0.233043003	0.214476003	0.202575	0.221927003	0.204667
R (A.W^{-1})					
-0.40000001	0.463504007	0.459108007	0.427571	0.443748007	0.415464
0.400000006	0.233043003	0.214476003	0.202575	0.221927003	0.204667

3. Results

In this work, Al/p-Si/TiO:NiO/Al photodetectors were produced and diode parameters, photovoltaic and photoresponsivity characteristics were investigated. Current-Voltage characteristics confirm that Al/p-Si/TiO:NiO/Al structures illustrate photodiode characteristics. Diode parameters such as series resistance, ideality factor, barrier height, and shunt resistance were affected by external illumination, but no direct illumination intensity-related correlation was evidenced. Ideality factor and barrier height values were found to be coherent with previous reports and within the acceptable range. Lastly, photoresponsivity characteristics were investigated and it was seen that responsivity changes with changing illumination intensity.

Acknowledgement

I would like to thank Dr. Ayşegül Dere and Prof. Dr. Fahrettin Yakuphanoğlu, for their support in this work. I also would like to acknowledgethe support of Kirklareli University Scientific Research Coordination Office with project number 230 (KLUBAP 230).

References

[1] Y. Takaoka, T. Sakamoto, S. Tsukiji, M. Narazaki, T. Matsuda, H. Tochio, M. Shirakawa, I. Hamachi, Self-assembling nanoprobes that display off/on 19F nuclear magnetic resonance signals for protein detection and imaging, Nat. Chem. 1 (2009) 557–561. doi:10.1038/nchem.365.

[2] N. Aslan, M.M. Koç, A. Dere, B. Arif, M. Erkovan, A.G. Al-Sehemi, A.A. Al-Ghamdi, F. Yakuphanoglu, Ti doped amorphous carbon (Al/Ti-a:C/p-Si/Al) photodiodes for optoelectronic applications, J. Mol. Struct. 1155 (2018) 813–818. doi:10.1016/j.molstruc.2017.11.050.

[3] F.J. González, B. Ilic, J. Aida, G.D. Boreman, Antenna-coupled infrared detectors for imaging applications, IEEE J. Sel. Top. Quantum Electron. 11 (2005) 117–120. doi:10.1109/JSTQE.2004.841474.

[4] A. Dere, M. Soylu, F. Yakuphanoglu, Solar light sensitive photodiode produced using a coumarin doped bismuth oxide composite, Mater. Sci. Semicond. Process. 90 (2019) 129–142. doi:10.1016/j.mssp.2018.10.009.

[5] A. Mekki, A. Dere, K. Mensah-Darkwa, A. Al-Ghamdi, R.K.K. Gupta, K. Harrabi, W.A.A. Farooq, F. El-Tantawy, F. Yakuphanoglu, Graphene controlled organic photodetectors, Synth. Met. 217 (2016) 43–56. doi:10.1016/j.synthmet.2016.03.015.

[6] P.D. Rack, P.H. Holloway, The structure, device physics, and material properties of thin film electroluminescent displays, Mater. Sci. Eng. R Reports. 21 (1998) 171–219. doi:10.1016/S0927-796X(97)00010-7.

[7] D. Ponnusamy, A.K. Prasad, S. Madanagurusamy, CdO-TiO2 nanocomposite thin films for resistive hydrogen sensing, Microchim. Acta. 183 (2016) 311–317. doi:10.1007/s00604-015-1653-y.

[8] K.C. Liddiard, Thin-film resistance bolometer IR detectors, Infrared Phys. 24 (1984) 57–64. doi:10.1016/0020-0891(84)90048-4.

[9] S. Özden, M.M. Koc, Spectroscopic and microscopic investigation of MBE-grown CdTe (211)B epitaxial thin films on GaAs (211)B substrates, Appl. Nanosci. 8 (2018) 891–903. doi:10.1007/s13204-018-0727-7.

[10] M. Mahdi, A. Djabri, M.M. Koc, R. Boukhalfa, M. Erkovan, Y. Chumakov, F. Chemam, Ab initio study of GdCo5 magnetic and magneto-optical properties, Mater. Sci. Pol. 37 (2019) 182–189. doi:10.2478/msp-2019-0017.

[11] M. Erkovan, M.E. Aköz, U. Parlak, O. Öztürk, The Study of Exchange Bias Effect in PtxCo1−x/CoO Bilayers, J. Supercond. Nov. Magn. 30 (2017) 2909–2913. doi:10.1007/s10948-017-4127-0.

[12] M. Yaqoob Khan, C. Bin Wu, M. Erkovan, W. Kuch, Probing antiferromagnetism in NiMn/Ni/(Co)/Cu3Au(001) single-crystalline epitaxial thin films, J. Appl. Phys. 113 (2013) 023913. doi:10.1063/1.4775575.

[13] M.M.K. Mustafa İlhan, Infrared Sensing Properties of Quaternary Cu2CoSnS4 Photodetectors, J. Mater. Electron. DEVICES. 1 (2020) 19–24.

[14] M. İlhan, M.M. Koç, B. Coşkun, A. Dere, F. Yakuphanoğlu, Structural and optoelectronic characterization of Cu2CoSnS4 quaternary functional photodetectors, Optik (Stuttg). 212 (2020) 164724. doi:10.1016/j.ijleo.2020.164724.

[15] M. İlhan, M.M. Koç, B. Coşkun, F. Yakuphanoğlu, Optical, Electrical and Photoresponsive Properties of Cu2NiSnS4 Solar Detectors, J. Electron. Mater. 49 (2020) 4457–4465. doi:10.1007/s11664-020-08197-5.

[16] M. Soylu, B. Coskun, A.G. Al-Sehemi, A.A. Al-Ghamdi, F. Yakuphanoglu, The validity of Kohlrausch law for the photocurrent transient and the role of N2/Ar flow ratio in photoconductivity of sputtered CoZnO, J. Alloys Compd. 712 (2017) 152–163. doi:10.1016/j.jallcom.2017.04.041.

[17] F. Yakuphanoglu, Transparent metal oxide films based sensors for solar tracking applications, Compos. Part B Eng. 92 (2016) 151–159. doi:10.1016/j.compositesb.2016.02.039.

[18] M. İlhan, M.M. Koç, B. Coşkun, M. Erkovan, F. Yakuphanoğlu, Cd dopant effect on structural and optoelectronic properties of TiO2 solar detectors, J. Mater. Sci. Mater. Electron. 32 (2021) 2346–2365. https://link.springer.com/article/10.1007/s10854-020-05000-3 (accessed March 9, 2021).

[19] S.J. Ippolito, S. Kandasamy, K. Kalantar-Zadeh, W. Wlodarski, Hydrogen sensing characteristics of WO3 thin film conductometric sensors activated by Pt and Au catalysts, in: Sensors Actuators, B Chem., Elsevier, 2005: pp. 154–158. doi:10.1016/j.snb.2004.11.092.

[20] R. Yang, J. Leisch, P. Strasser, M.F. Toney, Structure of dealloyed PtCu3 thin films and catalytic activity for oxygen reduction, Chem. Mater. 22 (2010) 4712–4720. doi:10.1021/cm101090p.

[21] A. Djabri, M. Mahdi, R. Boukhalfa, M. Erkovan, Y. Chumakov, F. Chemam, Structural, Magnetic, and Magneto-Optical Properties of Fe/Cu Superlattices, J. Supercond. Nov. Magn. 30 (2017) 3207–3214. doi:10.1007/s10948-017-4128-z.

[22] B.A.H. Ameen, A. Yildiz, W.A. Farooq, F. Yakuphanoglu, Solar Light Photodetectors Based on Nanocrystalline Zinc Oxide Cadmium Doped/p-Si Heterojunctions, Silicon. 11 (2019) 563–571. doi:10.1007/s12633-017-9656-4.

[23] A. Sharma, B.K. Lee, Photocatalytic reduction of carbon dioxide to methanol using nickel-loaded TiO2 supported on activated carbon fiber, Catal. Today. 298 (2017) 158–167. doi:10.1016/j.cattod.2017.05.003.

[24] Z. Jiang, J. Xie, D. Jiang, X. Wei, M. Chen, Modifiers-assisted formation of nickel nanoparticles and their catalytic application to p-nitrophenol reduction, CrystEngComm. 15 (2013) 560–569. doi:10.1039/c2ce26398j.

[25] M. Erkovan, Y.A. Shokr, D. Schiestl, C.B. Wu, W. Kuch, Influence of NixMn1−x thickness and composition on the Curie temperature of Ni in NixMn1−x/Ni bilayers on Cu3Au(001), J. Magn. Magn. Mater. 373 (2015) 151–154. doi:10.1016/J.JMMM.2014.02.017.

[26] A. Kösemen, Z. Alpaslan Kösemen, B. Canimkubey, M. Erkovan, F. Başarir, S.E. San, O. Örnek, A.V. Tunç, Fe doped TiO2 thin film as electron selective layer for inverted solar cells, Sol. Energy. 132 (2016) 511–517. doi:10.1016/j.solener.2016.03.049.

[27] M. Koç, N. Aslan, M. Erkovan, B. Aksakal, O. Uzun, W. Aslam, F. Yakuphanoğlu, Electrical characterization of solar sensitive zinc oxide doped-amorphous carbon photodiode, Optik (Stuttg). 178 (2019) 316–326. doi:https://doi.org/10.1016/j.ijleo.2018.10.008.

[28] N. Kurnaz Yetim, N. Aslan, M.M. Koç, Structural and catalytic properties of Fe3O4 doped Bi2S3 novel magnetic nanocomposites: P-Nitrophenol case, J. Environ. Chem. Eng. 8 (2020) 104258. doi:10.1016/j.jece.2020.104258.

[29] S. Özden, M.M. Koç, Wet-chemical etching of GaAs(211)B wafers for controlling the surface properties, Int. J. Surf. Sci. Eng. 13 (2019) 79. doi:10.1504/IJSURFSE.2019.102359.

[30] S. UYAR, B. COŞKUN, M. İLHAN, M.M. KOC, Optoelectronic Properties of ZnO:TiO2 Nanocomposite Thin Films, J. Mater. Electron. DEVICES. 5 (2021) 21–27. http://dergi-fytronix.com/index.php/jmed/article/view/140 (accessed October 15, 2021).

[31] M.M. Koc, Photoelectrical properties of solar sensitive CuO doped carbon photodiodes, J. Mol. Struct. 1208 (2020) 127872. doi:10.1016/j.molstruc.2020.127872.